



HAL
open science

Status and plans of the Virgo gravitational wave detector

Raffaele Flaminio

► **To cite this version:**

Raffaele Flaminio. Status and plans of the Virgo gravitational wave detector. SPIE Astronomical Telescopes + Instrumentation 2020, Dec 2020, Online, United States. pp.1144511, 10.1117/12.2565418 . hal-03107929

HAL Id: hal-03107929

<https://hal.science/hal-03107929v1>

Submitted on 29 Nov 2021

HAL is a multi-disciplinary open access archive for the deposit and dissemination of scientific research documents, whether they are published or not. The documents may come from teaching and research institutions in France or abroad, or from public or private research centers.

L'archive ouverte pluridisciplinaire **HAL**, est destinée au dépôt et à la diffusion de documents scientifiques de niveau recherche, publiés ou non, émanant des établissements d'enseignement et de recherche français ou étrangers, des laboratoires publics ou privés.

PROCEEDINGS OF SPIE

SPIDigitalLibrary.org/conference-proceedings-of-spie

Status and plans of the Virgo gravitational wave detector

Flaminio, Raffaele

Raffaele Flaminio, "Status and plans of the Virgo gravitational wave detector," Proc. SPIE 11445, Ground-based and Airborne Telescopes VIII, 1144511 (13 December 2020); doi: 10.1117/12.2565418

SPIE.

Event: SPIE Astronomical Telescopes + Instrumentation, 2020, Online Only

Status and plans of the Virgo gravitational wave detector

Raffaele Flaminio^{a*} for the Virgo Collaboration

^aLaboratoire d'Annecy de Physique des Particules (LAPP), Univ. Grenoble Alpes, Université Savoie Mont Blanc, CNRS/IN2P3, F-74941 Annecy, France

ABSTRACT

Virgo is a gravitational wave detector based on a 3 km long laser interferometer. After a first period of data taking between 2007 and 2011, a major upgrade called Advanced Virgo was prepared starting from 2009. After its implementation and commissioning Advanced Virgo started operation in 2017, joining the Advanced LIGO O2 run. In this period Advanced Virgo contributed to the first detection of gravitational waves from the binary neutron stars merger called GW170814. After a period of improvements and commissioning, in April 2019 Advanced Virgo started a new period of observation in coincidence with Advanced LIGO, during the so-called run O3. In the meantime, a new upgrade called Advanced Virgo Plus is being prepared. The first phase of this upgrade will be implemented at the end of O3 and completed by 2022, when the run O4 is planned to start. A second phase of upgrade is planned to be implemented between 2023 and 2024 and to be completed before the start of O5 in 2025.

Keywords: gravitational wave astronomy, gravitational wave detector, Virgo

1. INTRODUCTION

Virgo [1] is a gravitational wave detector based on a Michelson-type laser interferometer with arms 3 km in length. The construction of the detector was completed in 2003. The first data taking took place in 2007 in coincidence with the LIGO observatories [2]. While several observation runs were completed between 2007 and 2011, a major upgrade called Advanced Virgo [3] was approved in 2009.

Advanced Virgo started its first data taking in 2017 and participated in the first three-detectors joint detection on August 14th 2017 [4]. This detection led to the first localization of a gravitational source with a precision smaller than 100 square degrees. Three days later on August 17th 2017, Advanced Virgo participated in the first detection of gravitational waves from the coalescence of a binary neutron star [5]. This was the first gravitational wave identified and followed-up by tens of telescopes across all the bands of the electromagnetic spectrum, from radio waves to gamma rays, thus opening the field of multi-messenger astrophysics [6]. Since then, Advanced Virgo has participated into the observation run O3 together with the LIGO observatories from April 1st 2019 to March 31st 2020. During O3 the LIGO-Virgo network issued public alerts for gravitational wave candidate events at a rate approaching one per week. Recently the LIGO-Virgo collaboration published a catalog of all gravitational wave sources observed during O1, O2 and the first six months of O3 [7]. At the beginning of O3, Advanced Virgo sensitivity was such to allow the detection of the coalescence of binary neutron stars at distances of about 50 Mpc (averaged over the entire sky). Thanks to the commissioning activities performed during O3, the Advanced Virgo range for binary neutron stars reached up to 60 Mpc towards the end of O3.

Immediately after the end of the O2 run in 2017, the Virgo collaboration proposed an upgrade of Advanced Virgo named Advanced Virgo Plus (AdV+). In this paper, we describe the main features of AdV+, its design sensitivity and its timeline.

2. ADVANCED VIRGO PLUS (ADV+)

Since its first proposal in 2017, the AdV+ upgrade was conceived as a two phase's project. AdV+ Phase I and AdV+ Phase II.

AdV+ Phase I is currently under installation and should start operation during the next observation run O4. The current plan is to start O4 in 2022. The exact date will depend on the progresses in the implementation of both AdV+ Phase I and of the corresponding upgrades of the LIGO observatories. The goal for Phase I will be to be able to detect

gravitational waves from the coalescence of binary neutron stars at distances of the order of 100 Mpc. The detail spectral sensitivity is shown and discussed in Section 5.

Phase II is currently in the preparation stage. Its construction should start in 2021 and installation should follow at the end of O4 in 2023 so to be ready for the start of O5. The current plan is to start O5 in 2025. The goal for Phase II will be to be able to detect gravitational waves from the coalescence of binary neutron stars at distances of the order of 200 Mpc. The exact value will depend on the outcome of the R&D ongoing on low losses optical coating to reduce the mirror thermal noise. This is presented in Section 4. The details spectral sensitivity achievable with AdV+ Phase II is described in Section 5.

3. ADV+ PHASE I

AdV+ Phase I is focus on reducing and reshaping the effect of quantum noise. The origin of quantum noise in laser interferometers, like those used for gravitational wave detection, resides in the quantum nature of light. More precisely a detailed quantum analysis of a Michelson interferometer shows that quantum noise originates from the quantum vacuum fluctuations entering the interferometer from its output port. It is important to remind that during operation the interferometer output port is locked to the dark fringe. This corresponds to the interference condition in which only a small amount of the light injected into the interferometer reaches its output and most of the light is reflected back towards the input. As a gravitational pass through the interferometer, it changes the difference in length between the interferometer arms thus causing some of the laser field to leak at the output port. The detection of gravitational waves via a Michelson-type laser interferometer boils down to detect this electric field appearing at the dark port when a gravitational wave passes by.

When the interferometer is locked at the dark fringe, the vacuum fluctuations injected into the interferometer from the laser port do not reach the interferometer output port. Therefore, they do not have any practical effect on its sensitivity. The situation is different for the vacuum fluctuations entering from the output port. These fluctuations are reflected by the interferometer back to the output port (which is on the bright fringe for light entering from the output port). For this reason they affect directly the measurement of the field at the interferometer output port and so the ability to measure the interferometer arm length difference produced by a gravitational wave passing through the detector. In particular, since the measurement of the gravitational wave amplitude consists in measuring a phase difference between the two laser fields travelling in the two arms of the interferometer, the phase quadrature of the vacuum fluctuations limits directly the measurement. This is the so-called shot noise. It is a white noise (flat in frequency) always affecting the detectors sensitivity at the high frequency, typically above 100 Hz. Once expressed in terms of gravitational wave amplitude the shot noise tends to increase linearly with the frequency because of the response of the interferometer to gravitational waves. Indeed the interferometer response to a gravitational wave at high frequency decreases progressively due to the storage time of the light in the arms of the interferometer (which is of the order of a ms). This makes the effect of shot noise to increase linearly with frequency in terms of gravitational wave sensitivity.

The other consequence of quantum vacuum fluctuations is the radiation pressure noise. In this case, the amplitude quadrature of the vacuum fluctuations is at the origin of the noise. Indeed the vacuum amplitude fluctuations entering into the interferometer from the output port superpose with the incoming laser field and produce a fluctuation of the radiation pressure on the mirrors. Since these radiation pressure fluctuations are anti-correlated in the two arms, they produce a displacement of the interferometer mirrors that is indistinguishable from the effect of gravitational waves. Since interferometer mirrors are suspended to pendulums, they behave as free masses above the pendulums resonance (0.6 Hz in the case of Virgo). Consequently, the mirror inertia reduces the effect of radiation pressure noise at high frequency. For this reason, the radiation pressure noise is relevant at low frequency only; typically below 100 Hz.

A way to reduce the effect of quantum phase fluctuations (i.e. the shot noise) is to increase the laser power injected into the interferometer. This increases the field produced by the gravitational wave at the interferometer output port with respect to the quantum vacuum fluctuations. Indeed one of the goals of AdV+ is to increase the laser power injected into the interferometer from the present 25 W to at least 40 W. This will be done by introducing a new laser based on a fiber laser able to deliver 130 W. The laser wavelength will be the same as in Advanced Virgo i.e. 1064 nm. Moreover, an effort will be done to reduce the losses in the laser injection systems so to be able to inject at least 40 W into the interferometer. Among these, the most notable one will be the change of one of the input mode-cleaner mirrors to reduce the optical losses in the injection system (and to make its control easier). The increase of the laser power injected into the interferometer will push farther the needs for thermal compensation. This is required to overcome the increase in the

thermal load inside the cavity input mirror substrates. To this purpose, in AdV+ two different CO₂ lasers will be used for each input mirrors to compensate the thermal lens induced by the power transmitted through the mirrors. It must be noted that an increase in the laser power injected into the interferometer ends up increasing the radiation pressure noise thus reducing the sensitivity at low frequencies.

Another solution to reduce quantum noise is to inject squeezed vacuum states into the interferometer output port. These are vacuum states whose fluctuations in one of the two quadrature's are reduced at the expenses of larger fluctuations in the other. As an example, the fluctuations can be reduced in the phase quadrature at the expenses of larger amplitude fluctuations or, on the contrary, they can be reduced in the amplitude quadrature at the expenses of larger phase fluctuations. By adjusting the quadrature with reduced fluctuations, it is possible to reduce either the shot noise at high frequency or the radiation pressure noise at low frequency. Squeezed vacuum states were used for the first time in Advanced Virgo during the O3 run [8]. The system was tuned so to reduce the shot noise at high frequency. As expected, the radiation pressure at low frequency was slightly increased [9]. Nevertheless, the impact on the overall detector sensitivity from the larger radiation pressure noise at low frequency was smaller than the one coming from the reduction of the shot noise at high frequency. The reason for this was that the radiation pressure noise at low frequency was hidden by other noises mainly of technical origin. Overall, the detector sensitivity improved thanks to the use of squeezed states. As technical noises are reduced progressively and the laser power injected into the interferometer increases, it is expected that the impact of radiation pressure will become more and more important. The solution to avoid this effect is to implement a new type of squeezed vacuum states called frequency dependent vacuum squeezed states. These vacuum states have their fluctuations reduced in the amplitude quadrature at low frequency and in the phase quadrature at high frequency. In other words, the orientation of the vacuum fluctuations ellipse rotates by 90 degrees as the frequency increases. By properly choosing this transition frequency such as to coincide with the frequency where quantum noise shift from being radiation pressure noise dominated to shot noise dominated, it is possible to reduce both radiation pressure noise and shot noise i.e. to reduce quantum noise over the entire detector frequency band.

AdV+ will use frequency dependent squeezing to reduce quantum noise in a gravitational wave detector for the first time. This will be obtained by combining a squeezed vacuum source [8] with a 300 m long filter cavity. The squeezed vacuum state originated from the squeezed vacuum source is reflected from the 300 m long cavity. The cavity will be properly detuned so to have a rotation of the squeezing ellipse around 25 Hz. To achieve this goal the cavity finesse will be 10000. The initial goal for AdV+ Phase I will be to reduce the quantum noise by about 3 dB at high frequency without increasing the radiation pressure noise at low frequency. Later these performances will be improved during Phase II.

The optical configuration of AdV+ Phase I is shown in Figure 1. The implementation of frequency dependent squeezing in AdV+ foresees the installation of the squeezed vacuum source nearby the interferometer output port. From there the squeezed vacuum beam will be sent to the filter cavity by means of two suspended benches. The filter cavity will be placed along the north arm of the interferometer (in-line with the input laser direction). The beam reflected by the cavity will travel back through the same suspended benches and from there injected into the interferometer output port taking advantage of the Faraday Isolator there. Two additional Faraday Isolators will be placed on one of the two suspended benches. They will isolate the frequency dependent squeezed vacuum source from the main interferometer thus reducing the possibility that spurious light exiting the interferometer port can reach the frequency dependent squeezed vacuum source and being scattered back into the interferometer.

As usual for all systems involving the use of squeezed vacuum states, it is very important to reduce the optical losses as much as possible since losses degrade the squeezing. An effort will be made in AdV+ to reduce optical losses at the interferometer output port as well as in the frequency dependent squeezed vacuum source. This comprise the replacement of the two output mode-cleaners used in AdV with a single one having a larger finesse. This should allow reducing the losses of this part of the output optics from 5% to 2%. High quality mirrors with reflectivity's exceeding 99.99% and anti-reflection coatings with reflectivity's smaller than 100 ppm will be used throughout the system. In order to keep losses as low as possible, as in the case of Advanced Virgo, the photodiodes will have quantum efficiency equal to 99%.

In addition to frequency dependent squeezing, AdV+ will use signal recycling. This technique consists in adding a mirror at the interferometer output so to reinject the signal into the interferometer thus forming a new cavity called signal recycling cavity. By properly tuning the resonance conditions in this cavity, it is possible to reduce the quantum noise in part of the detector band while increasing it at other frequencies. AdV+ will use signal recycling in the so-called wideband configuration. In this configuration, both the shot noise at high frequency and the radiation pressure at low

frequency are reduced while the combination of the two noises at the intermediate frequencies increases. The major benefit of this technique will be to enlarge the detector bandwidth at high frequencies. This will allow reaching a better sensitivity with respect to the gravitational waves emitted by the coalescence of compact binaries during and immediately after the merger. These signals could provide crucial information about the neutron stars equation of state and black hole post-merger oscillations. The signal recycling mirror will have a transmission of 40%, this value being the result of a compromise between the detector band enlargement at high frequency, the increase of the quantum noise at intermediate frequencies and other issues related to the detector operation.

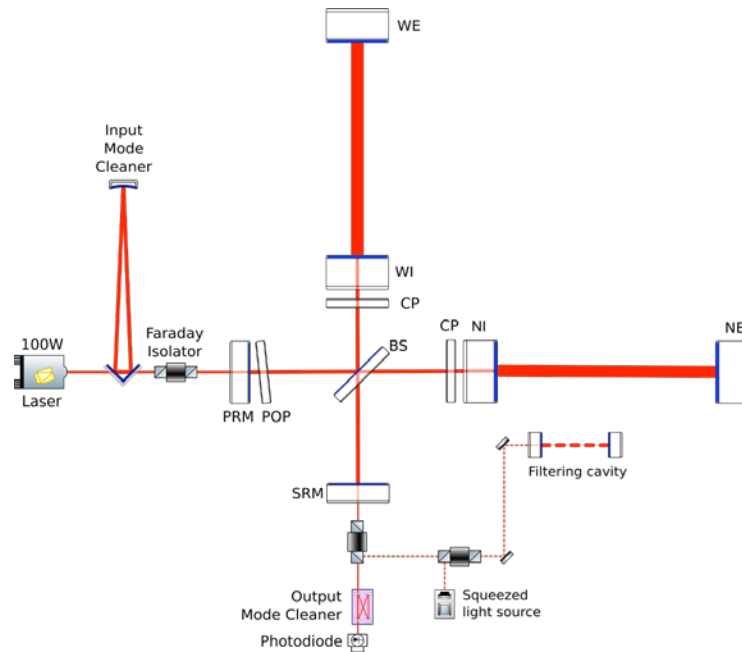


Figure 1. Sketch of the optical configuration of AdV+ Phase I. The most notable difference compared to Advanced Virgo are the use of signal recycling and of the filter cavity for the implementation of frequency dependent squeezing.

In addition to the upgrades described above to reduce quantum noise, AdV+ will be the occasion to implement several other upgrades aiming at reducing technical noises and at easing the detector operation.

First, the implementation of signal recycling will come with the installation of three auxiliary lasers to ease the interferometer operation. These lasers will operate at the double of the main laser frequency i.e. with a wavelength of 532 nm (in the green). Two will be placed in the terminal buildings and will be used to inject the green beams into the cavity arms from the back of the end mirrors. To realize these two beams a fraction of the main laser will be sent to the end building by means of two 3 km long fibers. There, a laser amplifier will amplify this light, which will then frequency doubled by a single pass second harmonic generator and finally phase modulated. The beams injected into the cavities from the back will be used to control the arm cavity length and ease the lock acquisition process i.e. the process that brings all the cavities that constitute the interferometer at their operating points.

In AdV+ Phase I several improvements are foreseen to reduce the effects of scattered light. Indeed, the light scattered out of the main beam by defects on the optical elements and that hits vibrating surfaces or suspended optics oscillating at low frequencies, may bring phase noise into the interferometer if it recombines with the main beam. To reduce this effect the AdV+ upgrade involve the installation of several diaphragms, baffles and beam dumps both at the output port and at the input port of the interferometer. In addition, an instrumented baffle will be added around one of the input mode-cleaner mirrors. This baffle will host an array of sensors to be able to measure the amount of scattered light around the mirror in the cavity. This will be the first time that such a technical solution will be implemented in Virgo. If successful, the plan for Phase II foresees to install similar baffles around the main interferometer mirrors in the 3 km arms.

Table 1. Main parameters of AdV+ during Phase I compared to the ones of Advanced Virgo during O3a

	Advanced Virgo during O3a	AdV+ Phase I
Laser & Injection		
Laser power	100 W	130 W
Power into the interferometer	18 W	40 W
Input mode-cleaner length	143 m	143 m
Input mode-cleaner finesse	1000	1000
Injection throughput	75%	85%
Modulation frequencies	6 MHz, 8 MHz, 56 MHz	6 MHz, 8 MHz, 56 MHz
Interferometer optical configuration		
Arm cavities length	3 km	3 km
Arm cavities finesse	450	450
Power recycling gain	39	39
Signal recycling	None	Yes
Mirrors		
Beam splitter	55 cm x 6.5 cm, 34 kg, T=50%	55 cm x 6.5 cm, 34 kg, T=50%
Input Test masses	35 cm x 20 cm, 42 kg, T=1.4%	35 cm x 20 cm, 42 kg, T=1.4 %
End Test masses	35 cm x 20 cm, 42 kg, T=5 ppm	35 cm x 20 cm, 42 kg, T=5 ppm
Power Recycling mirror	35 cm x 10 cm, 21 kg, T=5%	35 cm x 10 cm, 21 kg, T=5%
Signal recycling mirror	None	35 cm x 10 cm, 21 kg, T=40%
Detection		
Output mode-cleaner	Double cavity, Finesse = 120	Single cavity, Finesse = 1000
Detection losses	15 %	< 10%
Photodiodes quantum efficiency	99%	99%
Suspensions		
Mirror suspensions	Monolithic, fused silica fibers	Monolithic, fused silica fibers
Vibration isolation	Super-attenuators	Super-attenuators
Quantum noise reduction system		
Squeezed vacuum source	8 dB	12 dB
Filter cavity	None	L = 285 m, Finesse = 10000
Injection losses	11 %	< 10 %
Phase noise	120 mrad	40 mrad
Newtonian Noise Cancellation		
Sensors	None	Indoor seismic sensors
Noise reduction factor	n.a.	3

Finally yet importantly, AdV+ will host an array of seismic sensors around the main mirrors. In particular, during Phase I two arrays each made of 30 seismic sensors will be deployed around each of the end mirrors in the terminal buildings. A smaller test array will be deployed also in the cave under the main mirrors in the central building. The goal of these arrays is to measure precisely the seismic field around the mirrors. Using these measurements, it will be possible to subtract the effect of gravity gradient noise. The goal during phase I will be to test the principle that will then be implemented fully also in the central building during Phase II.

The main parameters of the AdV+ detector during Phase I are shown in Table 1. In the Table there are the corresponding values at the beginning of O3 (O3a). The sensitivity that AdV+ Phase I can reach if all the design parameters are achieved is shown in Figure 4 and discussed in Section 5.

4. ADV+ PHASE II

At intermediate frequencies, around 100 Hz where the noise spectral density is the lowest, AdV+ Phase I should allow reaching a sensitivity mostly limited by mirror thermal noise. The goal of AdV+ Phase II will be to improve the detector sensitivity by decreasing the limitation coming from the mirror thermal noise. This will be done by the two methods described here below.

The first method to decrease the impact of mirror thermal noise consists in changing the beam geometry inside the arm cavities so to increase the beam size on the end mirrors. Indeed the mirror thermal noise decreases when the beam size increases. A large beam will average the thermally driven mirror surface vibrations over a larger area thus reducing the amplitude of the thermal noise affecting the interferometer output. This is done while keeping the beam size on the input mirrors unchanged so that the degeneracy of the power recycling and signal recycling cavity is not worsened. It is important to remind that two decades of studies of mirror thermal noise have shown that the mechanical losses in the mirror reflective coatings are the main source of the mirror thermal noise. Since the end mirrors transmissivity is much smaller than the one of the input mirrors (few ppm vs 1.4%), their coatings are about twice as thick and so are the mechanical losses. For this reason, the end mirror thermal noise is predominant and increasing the beam size on end mirrors does decrease the total thermal noise considerably. For AdV+ Phase II the beam radius on the end mirror will increase from 58 mm to 91 mm bringing a reduction of the thermal noise at 100 Hz of about 25%. Such an improvement alone will double the rate of detectable binary neutron star mergers.

The second method consists in using coatings with lower mechanical losses. Reflective coatings are multilayers stack made of two different materials. One of the two materials has a higher refractive index and the other has a lower refractive index. At present both Advanced Virgo and Advanced LIGO mirrors use Ti:Ta₂O₅ as high index material and SiO₂ for the low index material. All the studies have shown that mechanical losses in the high index materials are considerably larger than in the lower index SiO₂ layers. For this reason, the high index materials dominate the coating total mechanical loss and research on the reduction of coating mechanical losses has been focusing on them. Several candidates are currently being investigated for the high index materials. The most promising solution so far are Silicon Nitrides and oxides based on Titania-Germania and Titania-Silica mixtures. The goal for AdV+ is to reduce the coating mechanical losses by a factor of three. By itself, this would bring a reduction of mirror thermal noise by about 40%. While reducing the coating mechanical losses, it is also important to keep the coating absorption in the range of 1 ppm (current coatings have absorption smaller than 0.5 ppm). This is important to avoid that the lensing effect induced by the thermal load in the cavity input mirrors raises to levels non-manageable by the thermal compensation system. The decision on the coating to be used in AdV+ Phase II should be made in 2021.

The optical configuration of AdV+ Phase II is shown in Figure 2. In order to manage the larger beams foreseen in AdV+ Phase II, the end mirror diameter should be large enough to reduce the amount of light clipped outside of the coating edge. AdV+ will use end mirrors 55 cm diameter and 20 cm thick for a total mass of 104 kg. The cavity input mirrors will remain the same size as now i.e. 35 cm diameter and 20 cm thick for a total mass of 42 kg. The radii of curvature (RoC), required to have a proper beam geometry inside the cavity, will be respectively 1969 m and 1067 m. This corresponds to a g-factor equal to 0.95 considerably larger than the one in Advanced Virgo (0.87). Nevertheless, simulations show that precisions on the RoC's similar to the ones demonstrated during the construction of the mirrors for Advanced Virgo will be sufficient to keep the cavity well within the stability region. The most stringent requirement will be on the differences between the RoC of the mirrors in the two arm cavities. This has to be smaller than 0.6m. While the mirror production process does not allow reaching such a small RoC difference, it is possible to achieve it after the mirrors installation using the ring heaters mounted around the mirror substrates. The same optical simulations show that

the polishing quality achieved for Advanced Virgo will allow keeping the intra-cavity losses within the required 75 ppm (same of Advanced Virgo) despite the cavity being closer to the instability boundary. The largest difference compared to Advanced Virgo will be a larger sensitivity to misalignments. Indeed, due to the larger g -factor the requirements on the tolerable misalignment will be about three times tighter than in Advanced Virgo. In particular, during the lock acquisition phase it will be necessary to keep the mirror aligned within 0.2-0.3 μrad . According to the experience with Advanced Virgo this is feasible.

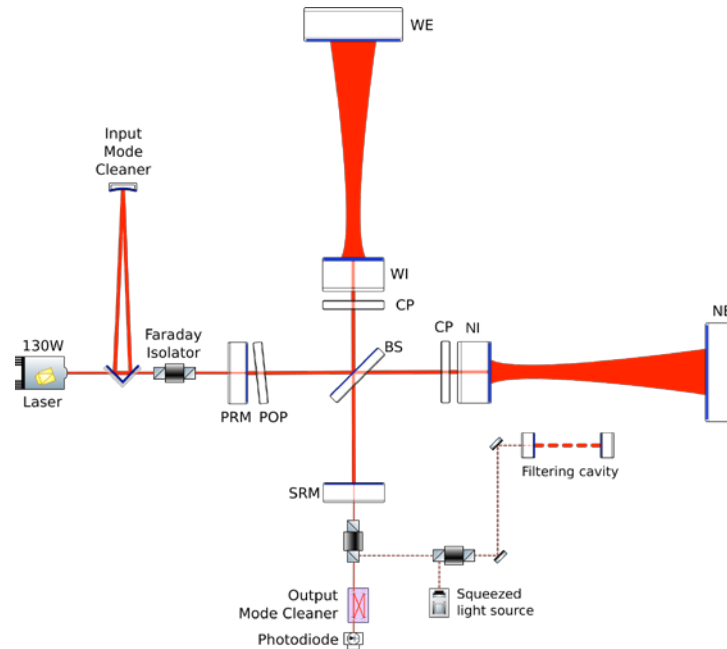


Figure 2. Sketch of the optical configuration of AdV+ Phase II. The most notable difference compared to AdV+ Phase I is the beam geometry inside the arms cavities.

Another consequence of the change of the beam geometry in the arm cavities is the need to redesign all telescopes used to extract the beams from the various interferometer output port. Preliminary designs were completed and do not show any particular difficulty. The most relevant difference will be for the telescopes used to extract the beam transmitted by the end mirrors. In this case, a converging lens will be polished directly on the back surface of the mirror to help the telescope realization.

The use of large mirrors mostly affects the suspensions and the seismic isolators (the so-called super-attenuators). Suspending a considerably larger diameter mirror involves the redesign of the payload i.e. the ensemble used to suspend the mirror with fused silica fibers and to control finely the mirror position. This redesign has been done and a prototype is currently being built. The new payload will weight around 500 kg to be compared with the current 300 kg. Such an increase in weight requires changing some of elastic element of the seismic isolators as well as some of the suspension wires. The anti-magnetic springs used in Virgo to reduce the vertical resonances and so improve the attenuation performances will have to be revisited as well. Nevertheless, the overall design and principle of the super-attenuators will remain unchanged and only the end mirror super-attenuators will be affected by these changes.

The main parameters of the AdV+ detector during Phase II are shown in the third and fourth columns of Table 2. The two different set of parameter corresponds to the so-called “high” and “low” configurations of AdV+ Phase II. They correspond to the worst and best sensitivity goals for Phase II that are shown in Figure 3.

As shown in Table 2, even if the focus of AdV+ Phase II is the reduction of the mirror thermal noise, an effort will be made to decrease further the effect of quantum noise further. This will be done by increasing the laser power injected into the interferometer to 80 W with a minimum goal of 60 W. In addition, the losses in the interferometer and in the

frequency dependent squeezed vacuum source will be reduced further in order to achieve 6 dB of squeezing with a minimum goal of 4.5 dB.

Moreover, during Phase II, AdV+ will complete the deployment of the seismic sensors arrays around all cavity mirrors. These will consist of 30 sensors in each terminal building (as for Phase I) and 60 sensors in the central building. The seismic data will be used to subtract the gravity gradient noise from the interferometer output. The goal will be to reduce gravity gradient noise by a factor of five with a minimum goal of a factor of three. This should be sufficient to make gravity gradient noise negligible compared to the suspension thermal noise.

5. ADV+ SENSITIVITY

The sensitivities planned for AdV+ Phase I and AdV+ Phase II are shown in Figure 3. For both Phases a “high” and “low” case is shown. These correspond to pessimistic and optimistic hypothesis made for the interferometer parameters during the observation runs. The two different set of parameters are given in Table 2.

The sensitivities achieved during O3 at the beginning of the observation run (O3a) and at the end (O3b) are shown on the same figure. As explained above, these sensitivities provided Advanced Virgo with the capability of detecting gravitational waves from coalescing binary neutron stars at distance of 50 Mpc and 60 Mpc respectively.

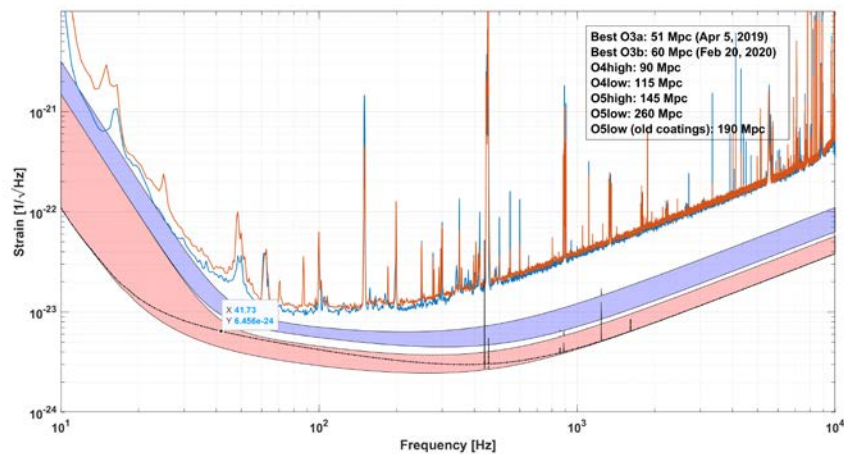


Figure 3. The range of sensitivities achievable by AdV+ Phase I (blue area) and AdV+ Phase II (pink area) is compared to the best sensitivities measured during O3a (first part of O3) and O3b (last part of O3). The dotted line within the pink area shows the best sensitivity achievable by AdV+ in case the same coatings used for Advanced Virgo are used also for AdV+ Phase II.

The blue area represents the range of possible sensitivities for Phase I (O4). The worst case correspond to the case where only 25 W are injected into the interferometer and a pure phase squeezing is used i.e. no frequency independent squeezing is operated during O4. In this case, the maximum distance at which a coalescing binary neutron star will be detectable will be 90 Mpc.

The best sensitivity achievable with AdV+ Phase I is shown in Figure 4. At low frequency, the O4 sensitivity is limited by a combination of technical noises represented by a simplistic function having a slope similar to what observed in the past. At higher frequencies, the limitation comes mainly from thermal noise and quantum noise. In this configuration, the maximum distance at which a coalescing binary neutron star will be detectable will be 115 Mpc.

The pink area in Figure 3 represents the range of sensitivities achievable during Phase II. The case “high” corresponds to the case where the same coatings used for Advanced Virgo are used for AdV+ Phase II. In this case, the improvement in the mirror thermal noise only comes from the larger beam size on the end mirrors. The “high” case considers that 60 W are injected into the interferometer. In this configuration, the maximum distance at which a coalescing binary neutron star will be detectable will be 145 Mpc. On the other hand, the “low” case assumes that the mirror thermal noise is decreased thanks to a reduction by a factor of three in the coating mechanical losses. This case also assumes that 80 W

are injected into the interferometer and that technical noises are made negligible at low frequencies. In this configuration, the maximum distance at which a coalescing binary neutron star will be detectable will be 260 Mpc. As shown in Table 1, other differences between these two configurations reside in the hypothesis on the quantum noise reduction due to the squeezing and on the gravity gradient noise reduction achieved by the Newtonian noise cancellation system.

Within the pink area, the dotted line represents the best sensitivity that one can achieve in case the same coatings used in Advanced Virgo will be used in AdV+ i.e. when all the other “high” parameters are considered. It is important to note that even if the AdV coatings are used, AdV+ Phase II still have the potential to reach a binary neutron star range of 190 Mpc.

Table 2. Main parameters of AdV+ during Phase I compared to the ones of Advanced Virgo during O3a

Parameter	O4 high	O4 low	O5 high	O5 low
Power injected	25 W	40 W	60 W	80 W
Signal recycling	Yes	Yes	Yes	Yes
Squeezing type	FIS	FDS	FDS	FDS
Squeezing detected level	3 dB	4.5 dB	4.5 dB	6 dB
ITM mass	42 kg	42kg	42 kg	42kg
ETM mass	42 kg	42kg	105 kg	105kg
ITM beam radius	48.7 mm	48.7 mm	48.7 mm	48.7 mm
ETM beam radius	58 mm	58 mm	96 mm	96 mm
Coating losses ETM	2.37e-4	2.37e-4	2.37e-4	0.79e-4
Coating losses ITM	1.63e-4	1.63e-4	1.63e-4	0.54e-4
Newtonian noise reduction	None	1/3	1/3	1/5
Technical noise	“Late high”	“Late low”	“Late low”	None
BNS range	90 Mpc	115 Mpc	145 Mpc	260 Mpc

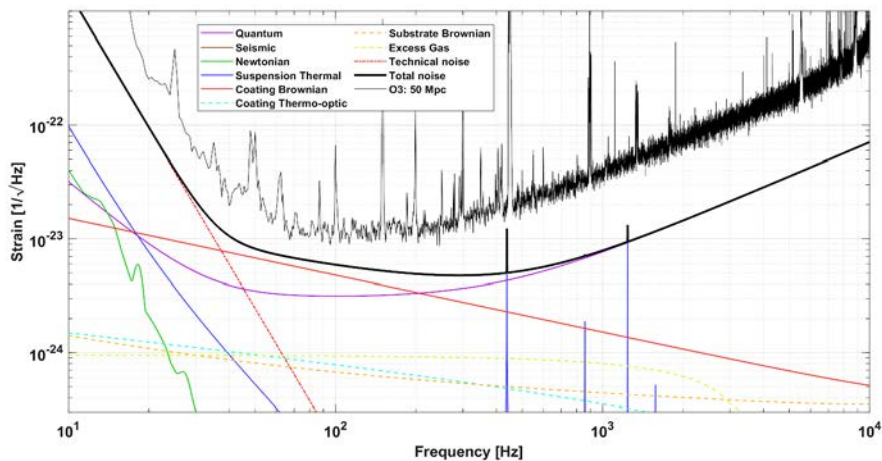


Figure 4. Anticipated best sensitivity of AdV+ during Phase I. For comparison, the sensitivity at the beginning of O3 is also shown. The larger bandwidth compared to O3a comes from the implementation of the signal recycling technique.

6. CONCLUSIONS

After two decades of research and development, the Advanced Virgo detector contributed to the first observation of gravitational waves from a binary neutron stars merger shortly after it entered into operation in 2017. The follow-up of this event with a wide range of telescopes opened the field of multi-messenger astronomy. Thanks to the improvement in the detectors sensitivity achieved since 2017, during O3 the LIGO-Virgo networks provides many new gravitational wave signals emitted by the coalescence of binary black holes, binary neutron stars as well as mix black hole - neutron star system. These results shows the importance of improving the sensitivity of these detectors. The Virgo collaboration has established a plan to improve further the detector sensitivity. The next upgrade, called Advanced Virgo + (AdV+), will be deployed in two phases: Phase I to be implemented before the start of the next observation run (O4) in 2022 and Phase II to be completed by the start of O5 in 2025. The upgrades described in this paper will allow the detection of binary neutron stars at distances as far as 100 Mpc during O4 and have the potential to reach as far as more than 200 Mpc during O5.

REFERENCES

- [1] Accadia T. et al., "Virgo: a laser interferometer to detect gravitational waves", *Journal of instrumentation* 7, P03012 (2012)
- [2] Abbott B. P. et al., "LIGO: the Laser Interferometer Gravitational-Wave Observatory", *Reports on Progress in Physics* 72 (7), 076901 (2009)
- [3] Acernese F. et al., "Advanced Virgo: a second-generation interferometric gravitational wave detector", *Classical and Quantum Gravity* 32 (2), 024001 (2015)
- [4] Abbott B. P. et al., "GW170814: A Three-Detector Observation of Gravitational Waves from a Binary Black Hole Coalescence", *Physical Review Letters* 119, 141101 (2017)
- [5] Abbott B. P. et al., "GW170817: Observation of Gravitational Waves from a Binary Neutron Star Inspiral" *Physical Review Letters* 119, 161101 (2017)
- [6] LIGO collaboration, Virgo collaboration et al., "Multi-Messenger Observations of a Binary Neutron Star Merger", *Astrophys. J. Lett.* 848, L12 (2017)
- [7] Abbott B. P. et al., "GWTC-2: Compact Binary Coalescences Observed by LIGO and Virgo During the First Half of the Third Observing Run", arXiv:2010.14527v1 [gr-qc] 27 Oct 2020
- [8] Acernese F. et al., "Increasing the Astrophysical Reach of the Advanced Virgo Detector via the Application of Squeezed Vacuum States of Light", *Physical Review Letters* 123 (23), 231108 (2019)
- [9] Acernese, F. et al., "Quantum Backaction on Kg-Scale Mirrors: Observation of Radiation Pressure Noise in the Advanced Virgo Detector", *Physical Review Letters* 125 (13), 131101 (2020)